# CW laser damage testing of RAR nano-textured fused silica and YAG

Bruce D. MacLeod, Douglas S. Hobbs, Anthony Manni, Ernest Sabatino, David M. Bernot, et al.

Bruce D. MacLeod, Douglas S. Hobbs, Anthony Manni, Ernest Sabatino, David M. Bernot, Sage DeFrances, Joseph A. Randi, Jeffrey Thomas, "CW laser damage testing of RAR nano-textured fused silica and YAG," Proc. SPIE 10447, Laser-Induced Damage in Optical Materials 2017, 1044705 (23 November 2017); doi: 10.1117/12.2280498

SPIE.

Event: SPIE Laser Damage, 2017, Boulder, Colorado, United States

# CW laser damage testing of RAR nano-textured Fused Silica and YAG.

Bruce D. MacLeod*, Douglas S. Hobbs, Anthony D. Manni, and Ernest Sabatino III
TelAztec LLC, 15 A Street, Burlington, MA, USA 01803-3404

David M. Bernot, Sage DeFrances, Joseph A. Randi, Jeffrey Thomas
Penn State Electro Optics Center, 222 Northpointe Blvd, Freeport, PA 16229

## ABSTRACT

A study of the continuous wave (CW) laser induced damage threshold (LiDT) of fused silica and yttrium aluminum garnet (YAG) optics was conducted to further illustrate the enhanced survivability within high power laser systems of an anti-reflection (AR) treatment consisting of randomly distributed surface relief nanostructures (RAR). A series of three CW LiDT tests using the 1070nm wavelength, 16 KW fiber laser test bed at Penn State Electro-Optic Center (PSEOC) were designed and completed, with improvements in the testing protocol, areal coverage, and maximum exposure intensities implemented between test cycles. Initial results for accumulated power, stationary site exposures of RAR nano-textured optics showed no damage and low surface temperatures similar to the control optics with no AR treatment. In contrast, optics with thin-film AR coatings showed high surface temperatures consistent with absorption by the film layers. Surface discriminating absorption measurements made using the Photothermal Common-path Interferometry (PCI) method, showed zero added surface absorption for the RAR nano-textured optics, and absorption levels in the 2-5 part per million range for thin-film AR coated optics. In addition, the surface absorption of thin-film AR coatings was also found to have localized absorption spikes that are likely pre-cursors for damage. Subsequent CW LiDT testing protocol included raster scanning an increased intensity focused beam over the test optic surface where it was found that thin-film AR coated optics damaged at intensities in the 2 to 5 MW/cm$^2$ range with surface temperatures over 250C during the long-duration exposures. Significantly, none of the 10 RAR nano-textured fused silica optics tested could be damaged up to the maximum system intensity of 15.5 MW/cm$^2$, and surface temperatures remained low. YAG optics tested during the final cycle exhibited a similar result with RAR nano-textured surfaces surviving intensities over 3 times higher than thin-film AR coated surfaces. This result was correlated with PCI measurements that also show zero-added surface absorption for the RAR nano-textured YAG optics.

**Keywords**: Nano-Textures, Anti-reflection, Fused Silica, Motheye, CW, YAG, Surface Absorption, LiDT

## 1.0 INTRODUCTION

Lasers continue to be power scaled for applications ranging from medical, materials processing, fundamental science, and directed energy weapons. These lasers can either be pulsed for high peak power or continuous wave (CW) for constant output power. The Laser Induced Damage Threshold (LIDT) of optics within the laser system often becomes the limiting factor in ultimate achievable power levels. The surfaces of these components typically require functional treatments for wavelength filtering or anti-reflection (AR) that must survive sustained high-intensity laser operation. Thin film dielectric material coatings are typically employed to achieve these functions, however it is well documented that defects and absorption in the coatings substantially contribute to reduced power handling capability.

For pulsed lasers, the damage is often associated with dielectric breakdown at interfaces from the high electric fields in the laser beam. This surface effect is enhanced by absorption in the functional coatings, and by defects in both the coating and polished surface of the optic. The LIDT of coatings for pulsed applications is well researched, and is typically quoted when purchasing an optic or specifying a thin film coating deposition. A growing body of data has shown that the pulsed LiDT of fused silica optics can be increased up to 5 times that of thin-film AR coatings by replacing coatings with RAR nano-textures consisting of a random distribution of nanometer-scale features etched uniformly into the optic surfaces [1-5]. For CW laser operation, the LiDT of optics is typically dominated by thermal effects related to absorption in the functionalized surface coatings that leads to material ablation, melting, or thermally induced stress fractures in the bulk. RAR nano-textured optics eliminate surface absorption and should

* bdmacleod@telaztec.com; phone 1 781 229-9905; www.telaztec.com

Laser-Induced Damage in Optical Materials 2017, edited by Gregory J. Exarhos, Vitaly E. Gruzdev, Joseph A. Menapace, Detlev Ristau, MJ Soileau, Proc. of SPIE Vol. 10447, 1044705
 · doi: 10.1117/12.2280498

therefore survive much higher CW laser power. CW LiDT testing is not common due to the need for expensive laser systems capable of emitting a beam with high power and high spatial mode quality that can be focused to the intensity levels needed to damage durable materials such as fused silica and yttrium aluminum garnet (YAG). One such CW laser damage system has been developed by the Pennsylvania State University Electro Optic Center (PSEOC) and utilizes a 1070nm wavelength fiber laser with 16 KW of output power. The results of four cycles of CW LiDT testing at PSEOC are described below comparing the survivability of fused silica and YAG optics incorporating RAR nano-textures to optics utilizing thin-film AR coatings. For each test cycle, sensitive surface absorption measurements made by the Common-path Photothermal Interferometry (PCI) method are correlated with the observed CW LiDT.

## 2.0 RAR NANO-TEXTURE FABRICATION AND MEASURED PERFORMANCE

RAR nano-textures are fabricated using a sequence of steps that are quite similar to the steps for depositing thin-film AR coatings. As-polished optics are cleaned and placed into a carrier fixture that is loaded into the plasma etch tool vacuum chamber. A proprietary, patented RAR nano-texture etch recipe is then initiated under computer control. Typical cycle time for nano-texturing a batch of fused silica optics is about 20 minutes– much faster than the typical multi-hour thin-film AR coating deposition cycles. Note that the RAR nano-texture etch process removes material uniformly from the optic surface, which in effect supplements the original mechanical polish. This in-situ "plasma-polish" provides another key benefit of RAR nano-texturing- the removal of surface contamination and most sub-surface damage from polishing that are the pre-cursors of damage. With thin film coatings, both subsurface damage from polishing, and contamination not removed in cleaning prior to coating remain buried under the film for the lifetime of the optic.

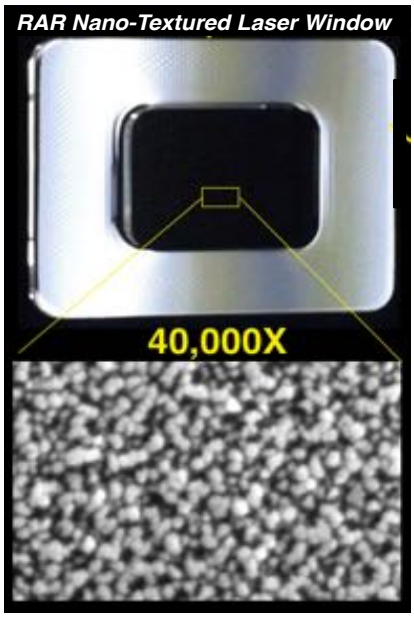


The graded index optical function introduced by RAR nano-texturing enables unprecedented optical performance compared to thin-film AR coating that rely on interference effects. The functional bandwidth of RAR nano-textured fused silica is far greater than can be achieved with AR coatings, with average single-surface reflection losses below 0.1% over the UV through NIR spectral range from 0.2 to 0.9μm, or the visible-NIR range of 0.4-1.6μm, with losses as low as 0.01% (-40dB) at specified wavelengths. Off-axis performance is also superior for graded index surface textures, with negligible reflection change seen from +/-30°, and minimal effect from +/-60°, without the color shift that is characteristic of thin-films. By precisely controlling the plasma etch parameters, the spacing between nano-texture features is kept sub-wavelength in the band of interest to avoid scattering losses.

RAR nano-textured samples prepared for the CW laser damage testing typically measured at less than 0.1% single surface reflection at the test wavelength of 1070nm. Figure 1 shows typical single surface reflection of untreated (black), RAR nano-textured (green), and thin-film coated (red, dark red) fused silica used in the damage tests. Note the broadband nature of the RAR nano-textured window performance with reflection loss below 0.1% from 500nm thru 1100nm, rising slowly to 0.6% at 1500nm. Photographs of the three windows against a black background are inset in Figure 1 and illustrate the extreme performance of RAR nano-textured surfaces relative to coatings.

## 3.0 FUSED SILICA: ABSORPTION MEASUREMENTS

For CW lasers, thermal effects related to absorption are the most common mechanism that results in damage to optical components. To measure the 1064nm absorption of both substrates and their surfaces, the technique of Photothermal Common-path Interferometry (PCI) was employed through the services of Stanford Photothermal Solutions (SPTS). PCI uses a high power 1064nm pump beam at the wavelength of interest to locally heat the optic through absorption and produce a thermal lensing effect. A low power probe beam intersects the pump beam at the probe site to create an interference pattern due to the localized index change, with the absorption level calculated from the fringe spacing[19,20]. The overlap of the beams is scanned either longitudinally through the sample from front to back, or transversely across a surface.

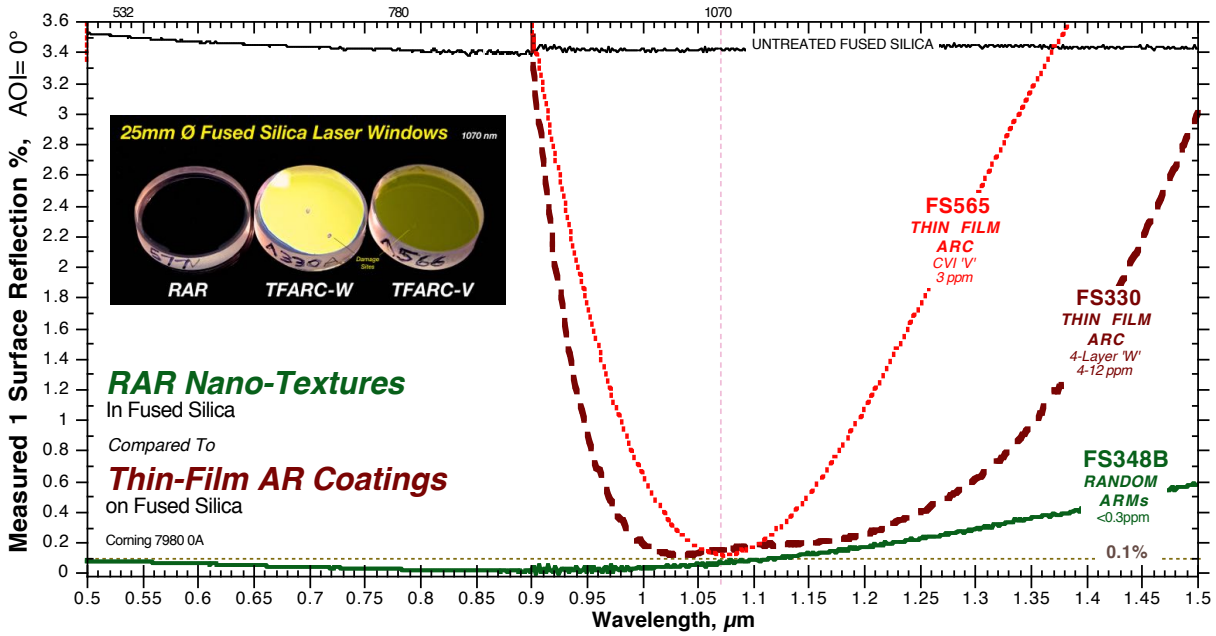


*Figure 1: Measured spectral reflectance of untreated, RAR textured, and thin-film AR coated CW damage test samples.*

Absorption measurements were made on most of the CW damage test samples, which included untreated, RAR nano-textured, and thin film coated fused silica. Bulk absorption is measured in units of parts per million per centimeter (ppm/cm), while for surface absorption the distance term drops and the units are simply in ppm. Figure 2 shows overlaid results for longitudinal PCI scans through several fused silica samples used in the CW damage test, as measured in units of bulk absorption.

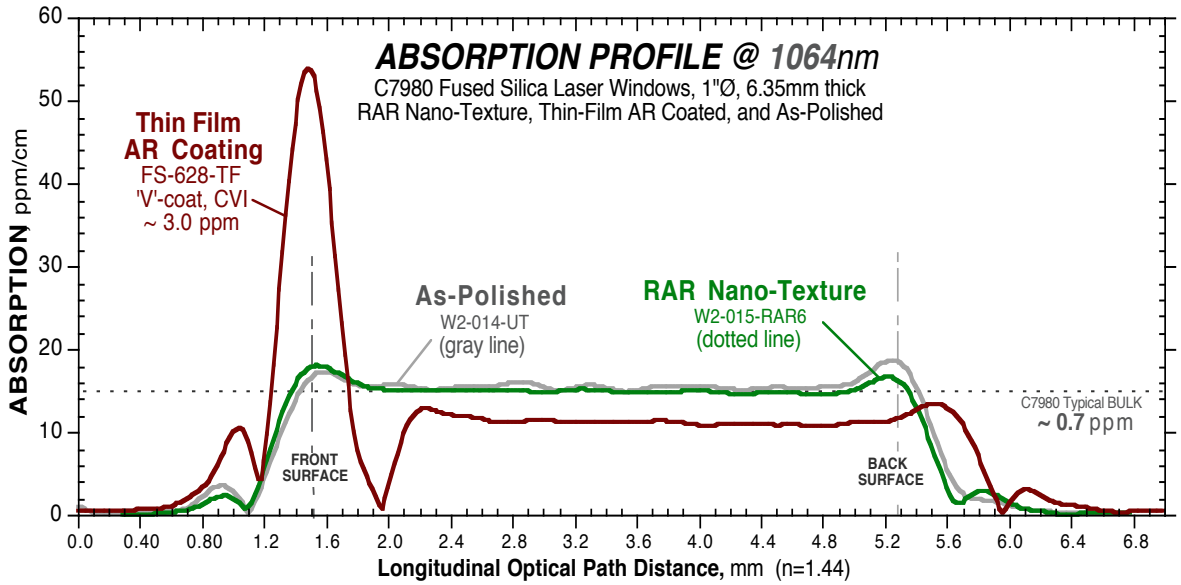


*Figure 2: Longitudinal CPI absorption scans through as-polished, RAR treated, and thin- film coated damage test samples.*

The Corning 7980 UV fused silica substrates show characteristic bulk values of 12-15 ppm/cm, as represented by the plateau between the front and back surfaces of each sample. Absorption spikes at the surfaces represent surface absorption only, and the magnitude of the spike is used to calculate surface absorption in ppm through a calibration

factor related to the test setup and the material index of refraction. The single-surface thin-film coated sample from CVI shows a large spike at the coated front surface, which corresponds to a film absorption level of 3.0 ppm. Neither the untreated or RAR nano-textured fused silica show evidence of a surface spike, which corresponds to an absence of surface absorption. Note that the small absorption bumps at the front and back surfaces of these samples are a measurement artifact related to the PCI beams intersecting the substrate/air interface.

Longitudinal absorption scans are not well suited for surface absorption measurements, as only a small area of each surface is sampled in the measurement. To get a greater understanding of surface absorption uniformity, the overlapped PCI measurement beams were transversely scanned across the surface of the substrates, instead of through the bulk as in Figure 2. Figure 3 shows the surface absorption result of 9mm long transverse scans across the surfaces of as-polished, RAR nano-textured, and thin-film AR coated samples. The background absorption level for the coating is constant across the surface at ~2.5 ppm; however many significant absorption spikes are revealed. These elevated absorption spots can produce extreme temperature rise under high irradiance, leading to a number of failure mechanisms. The untreated and RAR textured sample surface absorption levels are nearly constant across the surface, and the measured level between 0.5-0.7 ppm is related to bulk absorption and not surface absorption.

It should also be mentioned that the small surface absorption spikes observed on untreated and RAR nano-textured optics are typically minute levels of contamination related to inadequate cleaning. This has been revealed in cleaning tests on RAR textures, where these small absorption spikes are removed. Residual contamination on the air interface of RAR samples has the ability to be liberated or evaporated easily from the surface under high powers, whereas contamination entombed underneath a coating is typically permanent.

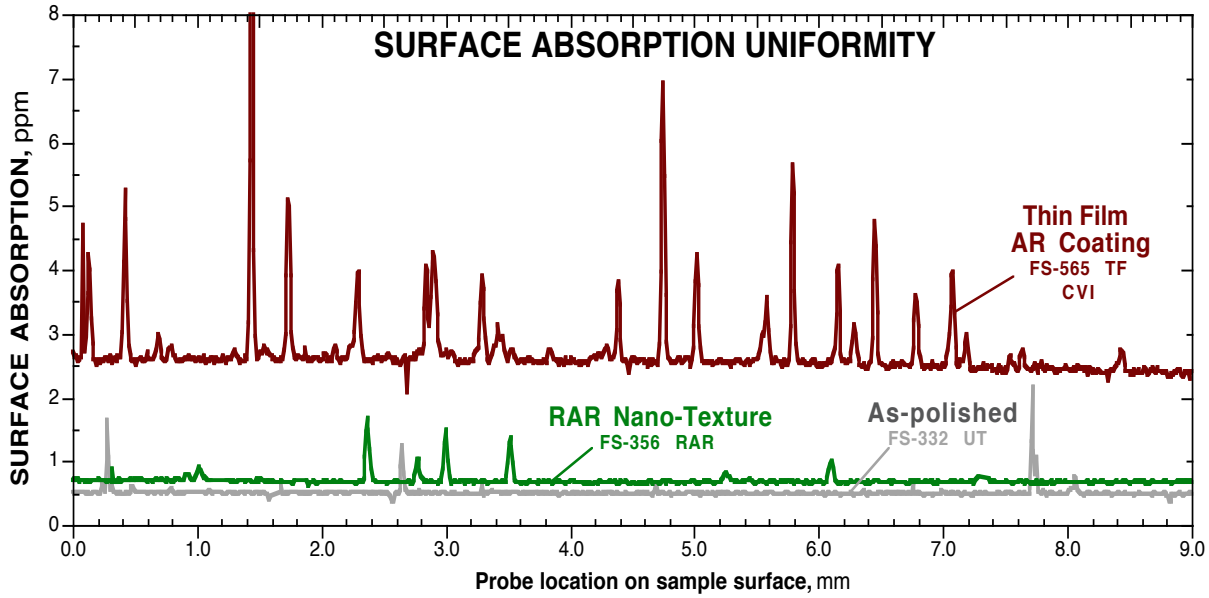


*Figure 3: Transverse CPI surface absorption scans through untreated (gray), RAR treated (green), and thin-film AR coated (maroon) CW damage test samples.*

## 4.0 FUSED SILICA: CW LASER DAMAGE TESTING

The CW laser damage testing of fused silica consisted of a series of three separate tests conducted by The Pennsylvania State University's Applied Research Laboratories Electro-Optics Center (PSEOC) over several years. An IPG Photonics Model YLS17000 Fiber laser capable of 17kW of CW output power at 1070nm was used for the High Energy Laser (HEL) damage testing sessions. The laser's collimating lens was mounted at a fixed position and the output beam was focused through a 2-inch diameter, 1 meter focal length fused silica lens. This lens is mounted to a translation stage to set the beam size at the target plane. A Mikron 7600 thermal camera was positioned to provide the best possible images, without risking exposure or damage to the camera during a catastrophic failure of an optic. Thermal videos were recorded for each laser shot or scan, and analysis of the thermal data was completed after the testing using an EOC developed software and the standard camera software.

The beam diameter at $1/e^2$ was measured using a Primes Focusing Monitor. The tool uses a spinning head with a 20um hole to collect a small portion of the beam and divert that energy to a detector. The spinning head reduces the amount of time that the tip is exposed to radiation, allowing the system to measure beams with high irradiance. The system is capable of measuring up to 5 MW/cm$^2$. The tip is continuously rotating and moving along the beam profile X-axis, stitching together the data to create the beam profile. The Primes provides information about the geometry of the beam, the location of the beam in space, the beam parameter product, and M2 beam quality. The focusing monitor was placed at the target test plane and the laser beam was measured using laser power levels that resulted in a peak irradiance of less than 1 MW/cm$^2$. The beam profile does not change with power; therefore, once the beam profile is determined, the laser power setting determines the exposure intensity. The profile was measured after each scan session and verified that the beam profile had not changed, as shown in the image on the right. Through the series of three damage tests, protocol was modified to increase power density, areal sampling technique, and laser bench environment, as noted in each test section below.

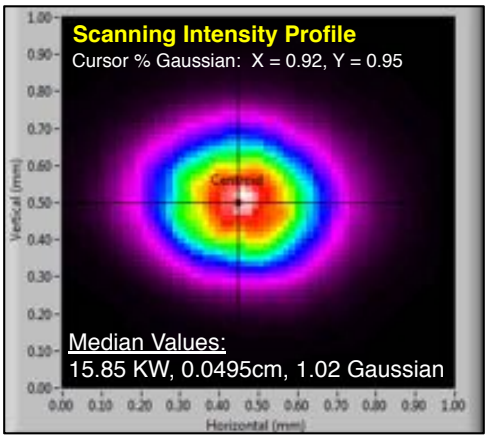


The fused silica substrates used in all tests were 1" diameter, ¼" thick Corning 7980 Grade 0A, with precision polished 10-5 scratch-dig and λ/10 flatness surface quality. Thin-film AR coatings were specified as high damage threshold, laser grade quality and designed for minimum reflectivity at 1064nm. Prior to shipment to PSEOC for testing, RAR textured and as-polished optics were acid cleaned, while thin-film coated samples were solvent rinsed. At PSEOC, the samples were blown off with clean air to remove loose debris before testing. Samples were installed into standard 1-inch non-adjustable mounts with the surface to be tested aligned as the beam entrance face. In order to determine laser position on the optic, a red guide beam was co-aligned to the 1070nm laser during measurement.

### 4.1 First Test, Static

The first test of RAR nano-textured fused silica optics employed a static five-spot test pattern, which was the same for each sample. The beam was focused to a spot diameter of 1.0mm, which produced a maximum power density of 3.0 MW/cm$^2$. A graphite beam dump was placed beyond the sample and an exhaust system was placed approximately 6 inches away from the test optic, which provided approximately 400 FPM of draw across the optic. The exhaust pulls any debris and contaminates away from the optical test surface during the experiments. The power was ramped in 0.5 MW/cm$^2$ increments with 30 sec dwell times, up to 3.0 MW/cm$^2$. Thermal imaging recorded sample temperature at each power level, and samples were monitored for evidence of laser-induced damage. Six 25.4mmØ x 3.1mm thick fused silica samples were tested: two as-polished, two RAR nano-textured, one Motheye textured, and one high damage threshold thin-film AR coated optic from Edmunds Optics.

No samples were damaged with the low power density used in this initial test, although interesting results were seen in the thermal measurements taken during illumination. The RAR nano-textured samples showed the same minimal heating as the untreated sample to a level around 48° C at the maximum power density of 3.0 MW/cm$^2$, indicating that the heating was solely due to bulk absorption. In contrast, the thin-film coated samples showed significantly more heating as the temperature ramped as high as 96°C. Figure 4 shows the thermal imaging results for three samples variants, noting sample temperatures after 30 second dwell at 3.0 MW/cm$^2$. Note that the thermal gradient colors auto-scale for min-max temperature range for each sample individually, such that the gradient levels between samples is not consistent.

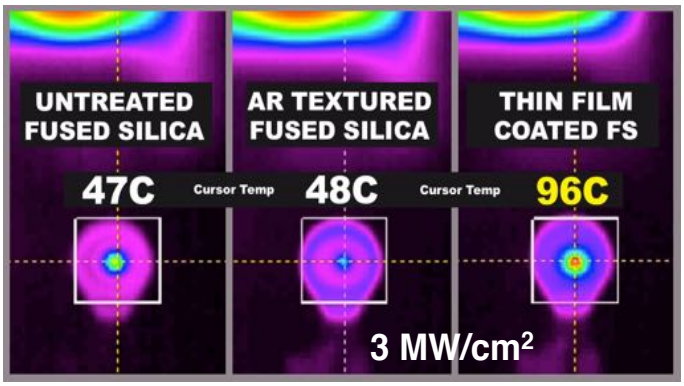


*Figure 4: Thermal images of untreated (left), RAR textured (middle), and thin film AR coated (right) samples, at onset of maximum power and after 30 seconds dwell.*

## 4.2 Second Test, Scanning

Several issues where identified in the 1st round of testing, including in sufficient power density, inadequate sampled surface area, and the cleanliness of the test environment. To increase power density, the beam was focused harder to 0.5mm diameter, which gave a maximum irradiance level of 14.5 MW/cm$^2$. The beam diameter was set by adjusting the sample plane with an Aerotech translation stage to precisely set the spot size. Power density levels were incremented through 1, 2, 5, 9, 11, and 15 MW/cm$^2$ steps for each sample unless damage occurred.

A much greater sampled area was attained for each optic through the implementation of a scanning stage, which allowed samples to be rastered during testing. This provided a more statistically relevant data set as bulk and surface defects stood a much greater chance of being intersected. Small diameter beams combined with static testing can give erroneously high damage thresholds; that have little real world merit. Ideally, the entire clear aperture on an optic would be incrementally illuminated to powers that induce failure, although lasers with sufficient power and beam quality for this type of test are not readily available.

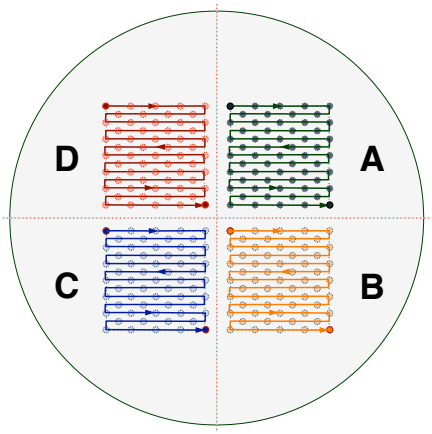


*Figure 5: 4-quadrant scanning beam pattern for CW laser damage tests.*

The raster areas were defined as four separate 5 x 5 mm areas, or quadrants, as shown in Figure 5. Velocities for the translation over this area was set to ensure the total scan time was 6 minutes for each quadrant scan, with a 24 minute total time for each power level per part. Total scan length at each power level with the serpentine raster pattern was 240mm per sample. The extended testing time required replacing the graphite beam dump with the use of the Primes power monitor as the beam dump to avoid graphite heating and potentially contaminating the samples under test. The device is water-cooled and monitors the output power of the laser during the test shots. The power monitor was placed about 2 meters away from the optical test component where the beam has diverged to sufficiently low levels. All other aspects of the testing were the same as those in the first testing session. Figure 6 shows the overhead layout of the CW laser damage testing setup with scanning sample stage.

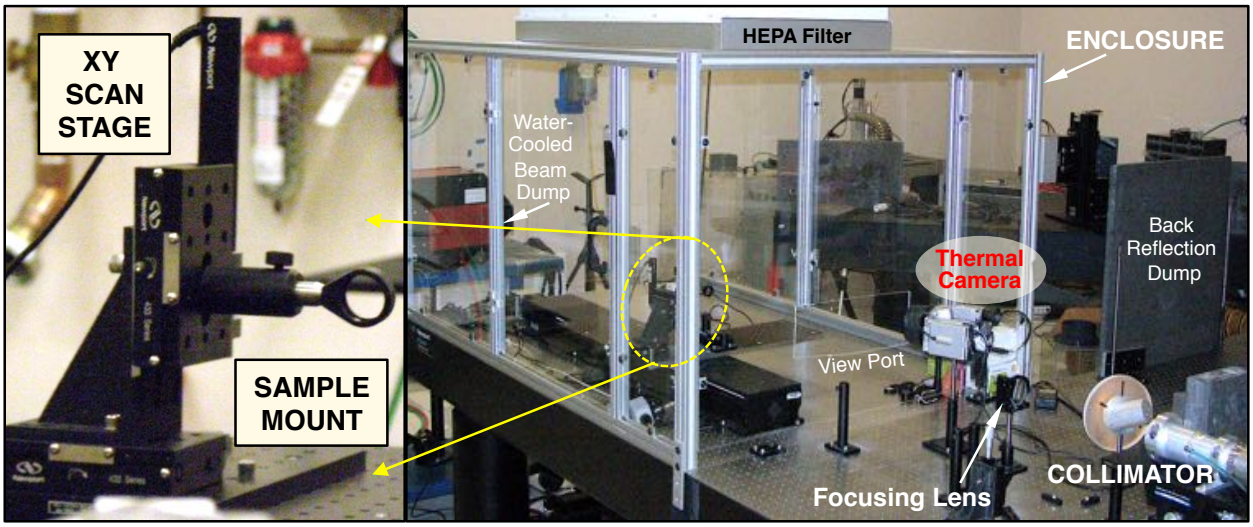


*Figure 6: Sample mount (left) and overview (right) of the CW laser damage test setup at PSEOC.*

The nine fused silica substrates included in the test were 25.4mmØ x 5.4-6.4mm thick, and the variants were: six RAR textured, two e-beam deposited thin-film AR coated from MIT Lincoln Laboratories (MITLL), and one e-beam deposited thin-film AR coating from CVI. Three RAR textured substrates were also given surface treatment variants: two substrates were given a super-hydrophobic treatment for anti-wetting properties, and one was given a hexamethyldisilazane (HMDS) treatment to produce a surface that is resistant to adsorption of hydrocarbons[21]. These ultra-thin surface texture treatments have been shown to have no effect on optical performance or surface absorption, and can increase a textured optics lifetime in applications with challenging environmental concerns.

The scanned results were much more revealing than the static testing, with the results tabulated in Figure 7. Power density is noted on the y-axis, and the sample IDs and AR treatment type are noted across the bottom of the plot. The solid bars for each sample represent the survived power density levels for the four quadrants. A solid red box notes power level where damage occurred.

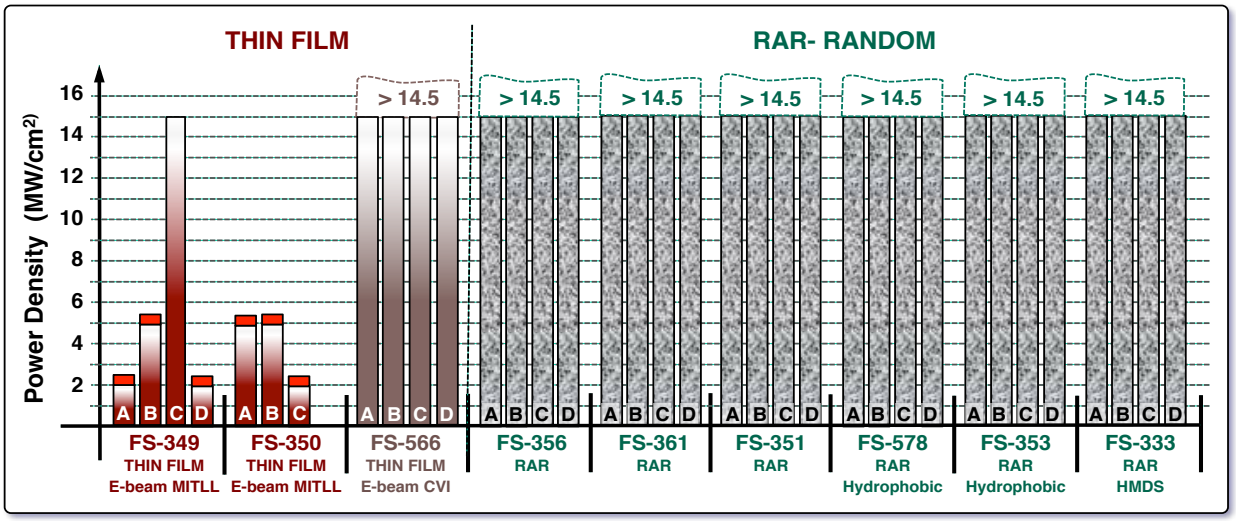


*Figure 7: 2nd TEST: 1070nm CW laser damage test results on RAR textured and thin-film AR coated fused silica.*

None of the six RAR nano-textured windows were damaged up to the maximum fluence of 14.5 MW/cm$^2$. Minimal substrate heating was observed under maximum irradiance, with the peak temperature of the 4 quadrants of all samples averaging 38°C. The super-hydrophobic and HMDS surface treatments had no adverse effect on the damage or thermal test results. One RAR sample (FS356) was observed to have surface contamination prior to test, so it was inadvertently cleaned with a drag wipe instead of the solvent rinse that is the cleaning protocol with nano-textures. The average peak quadrant temperature on this sample was 67°C, likely due to contamination from the drag wipe residing in the texture during test. Note that the standard cleaning procedure for RAR textures is to simply rinse the optics in solvents or a cleaning solution containing ammonia, although for heavily contaminated surfaces, a sulfuric acid based solution may be used, followed by de-ionized water rinse.

The two MITLL thin-film coated samples failed at variable power levels as low as 2 MW/cm$^2$, and exhibited extreme temperature spikes to greater than 250°C prior to failure. The thermal images on the left side of Figure 8 shows heating of the RAR texture at 14.5 MW/cm$^2$, and a thin-film AR coated sample near the onset of failure near 2 MW/cm$^2$. The photograph on the right side of Figure 8 shows an RAR nano-textured and a thin-film coated sample after testing. Note that there are multiple failures sites on the coated sample and the lower damage site near the label created significant material ejection. There is also a latent image of the scanning grid on upper half of the coated sample. The RAR treated sample on the left was unblemished and retained its extreme AR properties through the visible to the near IR range.

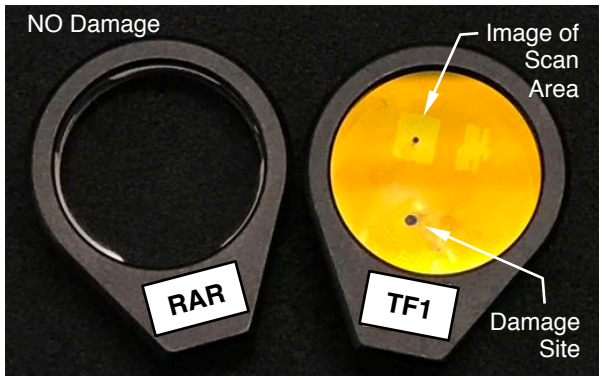


*Figure 8: Post-damage test photographs of RAR nano-textured and thin-film AR coated fused silica*

## 4.3 Third Test - Scanning

The third test repeated the use of the scanning stage, but replaced the debris exhaust near the sample with a HEPA filtered clean hood that provides about 100 CFM of downward airflow at the optic under test. The fiber laser output was slightly increased for the third test so that for the same 0.5mm diameter spot size, a maximum power density of

15.5 MW/cm$^2$ was attained. The number of irradiance levels was also increased to better define the damage thresholds. The test comprised of eight 25.4mm diameter x 6.4mm thick fused silica samples. The variants included one untreated (as-polished), three RAR textured, two e-beam thin-film AR coatings from CVI, and two ion-beam sputtered (IBS) thin-film AR coatings from MITLL. No environmental surface treatments were evaluated with the RAR textured samples.

The results of the third damage test are summarized in Figure 9**,** in the same plot layout as in Figure 7. As in the previous scanning test, all three Random textured substrates survived to the maximum power density of 15.5 MW/cm$^2$, with minimal heating effects compared to the as-polished sample W2-043.

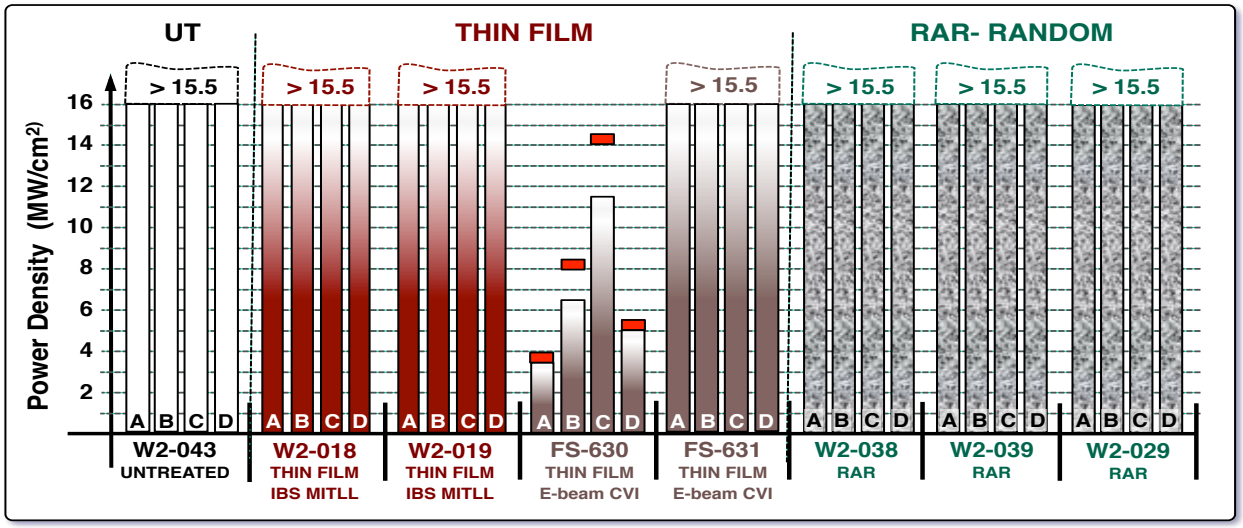


*Figure 9: 3rd TEST: 1070nm CW laser damage test results on untreated, thin-film coated, and RAR textured fused silica.*

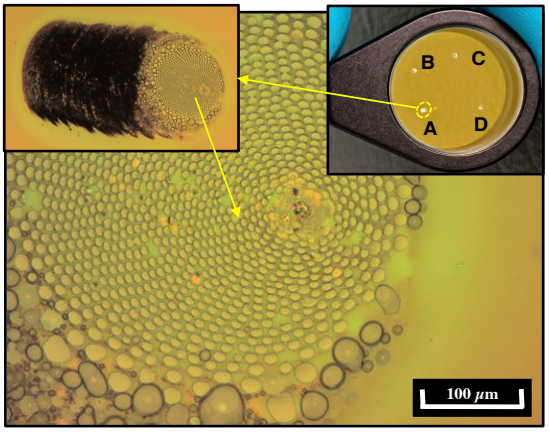


The two CVI thin-film coated samples showed mixed results; sample FS-630 failed in all four quadrants at various power densities, while sample FS-631 survived under maximum irradiance. The series of images on the right shows the nature of a typical failure site for sample FS-630, where the film appears to have lifted or melted. Both MITLL ion beam sputtered thin-film samples survived to 15.5 MW/cm$^2$ and did not show excessive heating, with average maximum quadrant temperature of 57°C which was higher than the RAR textured samples. The use of ion beam sputtering for depositing films for use in NIR lasers has shown promise, however the inherent nature of absorptive defects within films remains a concern.

The thin-film AR coated sample damage results were quite variable, from failure at levels as low as 2.0 MW/cm$^2$ to surviving to 15.5 MW/cm$^2$. This inconsistency is common with films and is attributed to random and localized absorption spikes caused by defects within the film. One observation from the scanning tests is that these thin-film absorption sites visually "light up" and temperature spike at low powers, before later failing under higher irradiance. In contrast, the damage tests showed very consistent results for the RAR treated samples- no damage was observed and substrate heating was minimal and similar to the untreated samples, confirming that the surface texture did not contribute to sample heating due laser irradiance. This correlates well with PCI measurements taken on the RAR textured fused silica samples, where no surface absorption is observed with the etched surface. This absence of surface absorption with surface textures manifests itself in producing far less thermal lensing than with coated optics, resulting in higher beam quality that is stable over time. This series of CW laser damage tests for evaluating AR treatments demonstrate that for high power CW laser systems, Random AR surface textures provide a superior non-absorbing, high power handling, and high reliability solution for fused silica laser components.

## 5.0 YAG: RAR BACKGROUND and MEASURED PERFORMANCE

Yttrium aluminum garnet or YAG crystals have favorable properties as gain media host material for high-power lasers. Common applications use neodymium doped YAG to provide strong emission at 1064nm, and ytterbium to emit at 1030nm. For CW laser applications, power scaling of YAG is limited by absorption in thin film AR coatings which can lead to catastrophic fracture of the crystal material. To date there has been little reported data on the CW laser damage testing of YAG. This work reports on the 1070nm CW laser damage testing of (111) oriented single crystal YAG sourced from Synoptics in Charlotte NC. The YAG surfaces were precision polished to 10-5 scratch/dig and 1/10 wave flatness. Both RAR nano-texturing and thin film AR coatings were applied to one surface of each sample. Thin-film AR coatings were deposited by Blue Ridge Optics (Lynchburg VA). Figure 10 shows the measured reflection of both RAR nano-textured and thin-film AR coated YAG used in the CW damage testing. The thin-film AR coating shows a reflectivity minimum of 0.07% at 990nm, while the RAR nano-textured YAG surface shows a 0.03% reflectivity minimum at 1070nm.

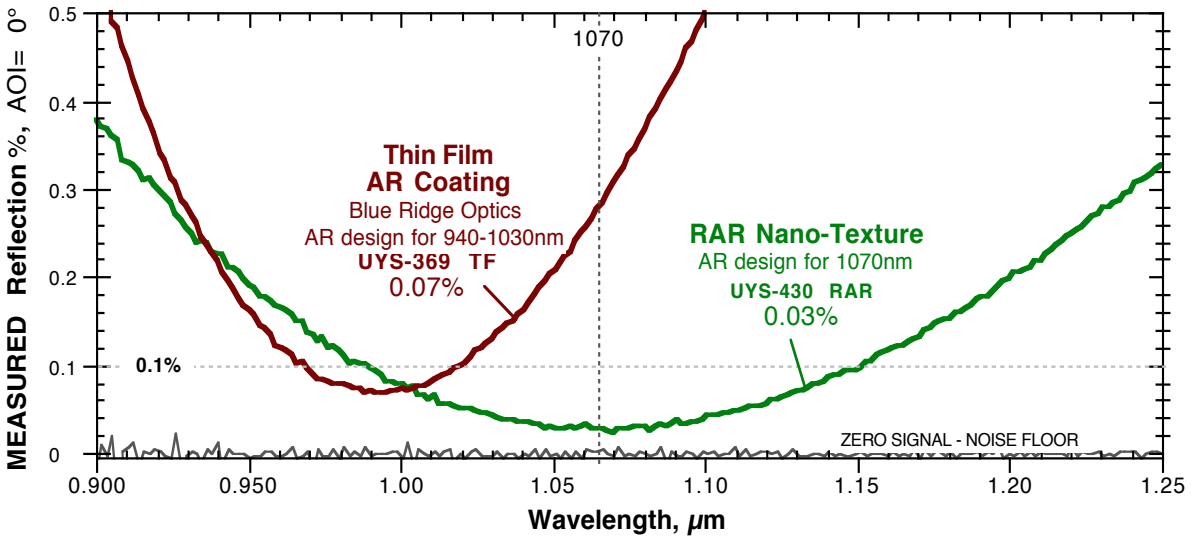


*Figure 10: Measured single surface reflection of RAR treated and thin-film AR Coated YAG.*

## 6.0 YAG: ABSORPTION MEASUREMENTS

Longitudinal absorption scans at 1064nm of untreated and AR treated YAG substrates were made with Photothermal Common-path Interferometry (PCI) by Stanford Photothermal Solutions (SPTS). All samples were measured for absorption as-received after polishing, and samples with elevated bulk or surface absorption were removed from the test batch. Substrates included in the damage tests showed bulk absorption levels of 40-75 ppm/cm, which is considered a typical range for undoped YAG. RAR nano-textured YAG substrates were measured again after RAR etching or thin film coating.

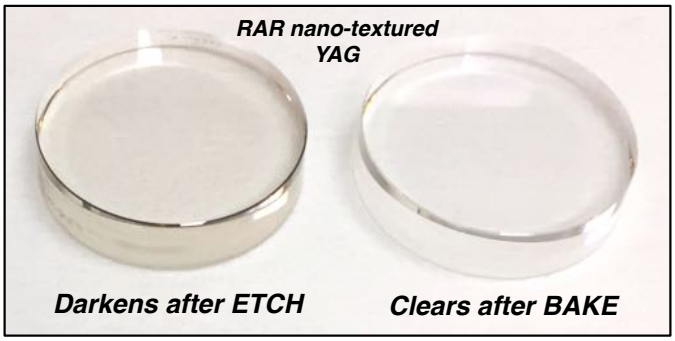


The visual appearance of the YAG after plasma etching the RAR texture showed an unexpected and distinctive light gray tinting. These RAR nano-textured samples were measured for absorption and were found to have a large increase in bulk absorption level to over 5000 ppm/cm- unsuitable for any laser application. It was apparent that the UV spectral lines from the reactive ion (RIE) etch plasma used in texturing the samples activated color centers in the YAG material. Varney and Selim identified oxygen vacancies and iron impurities as the main source of color centers in YAG. Color center activation is described as a process where defects or vacancies trap electrons, which can exist in different energy

levels within the trap, resulting in new absorption characteristics. However, it was also reported that air or oxygen-anneal at 400°C can eliminate color centers in YAG single crystals[22].

In an attempt to eliminate the plasma induced colors centers, RAR nano-textured YAG sample UYS-375 was baked at 400°C for 1 hour in an ambient oven, and upon cooling, had regained its original transparency as shown in the image on the right. The sample was measured by PCI and the bulk absorption was found to be over an order of magnitude lower at 370 ppm/cm. The sample was then baked at 460°C for 2 hrs, lowering the bulk absorption to 92 ppm/cm. A third bake at 480°C for 2 hrs lowered the bulk absorption to 50 ppm/cm, in line with the as-polished level of 65 ppm/cm. Figure 11 shows the absorption levels measured for the different bake profiles. All four RAR treated samples in the CW damage test were baked under the 480°C conditions, and were measured again to confirm the bulk absorption levels returned to as-polished measurement levels.

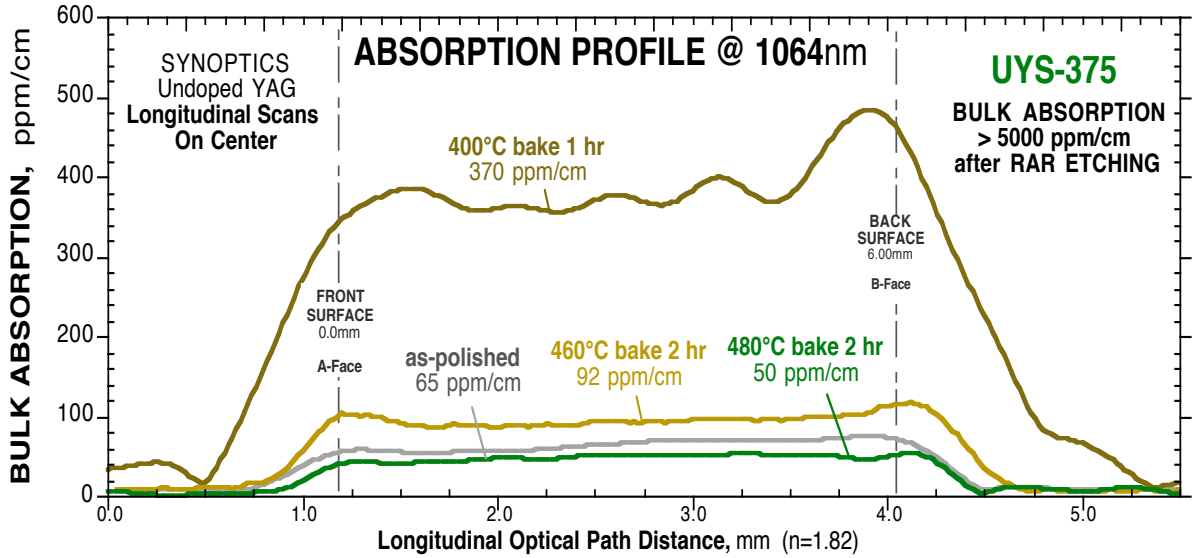


*Figure 11: PCI absorption measurements on RAR textured YAG showing effect of baking temperature on bulk absorption.*

The thin film coatings included in the CW test were also measured with PCI, and were found to have an absorption level of ~5 ppm. Figure 12 shows typical results for untreated, RAR textured, and thin-film AR coated YAG samples. Note that the absorption is shown on a log scale to provide more detail near the bulk levels.

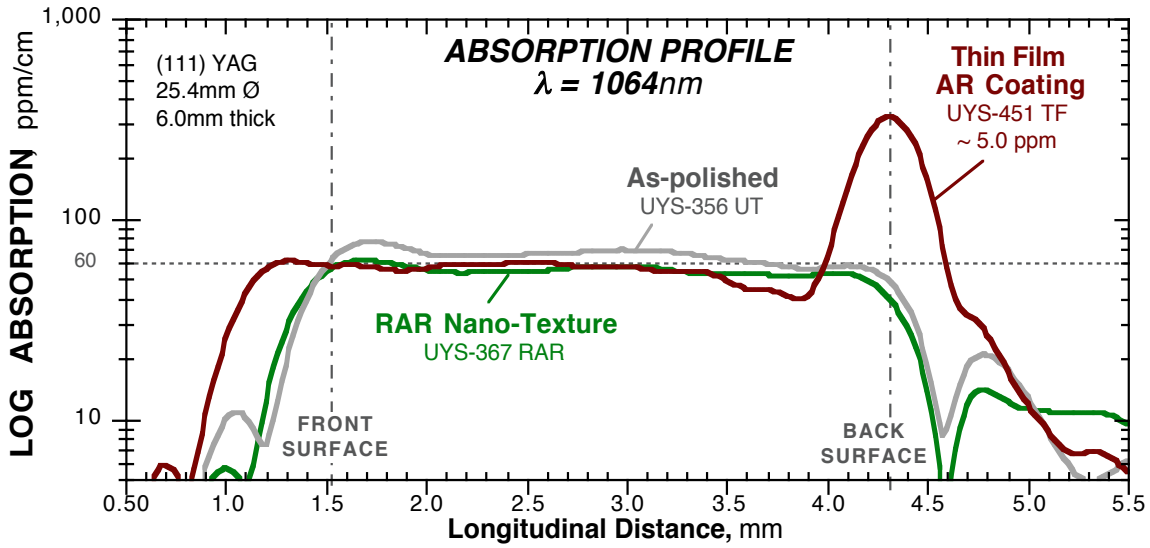


*Figure 12: Longitudinal PCI absorption measurements on untreated, RAR textured, and thin-film AR coated YAG.*

## 7.0 YAG: CW LASER DAMAGE TESTING

YAG samples were CW laser damage tested at PSEOC in series with third fused silica test described in section 4.3, with test protocol remaining the same, including four quadrant scanning with the 5mm x 5mm serpentine pattern. Nine YAG samples were tested, comprising of three untreated (as-polished), four RAR textured, and two thin-film AR coated YAG. The CW laser damage threshold of undoped single crystal YAG was expected to be in the range of 2-5 MW/cm$^2$, so testing was started at 1 MW/cm$^2$ and incremented in small 0.5-1.0 MW/cm$^2$ steps to better isolate the damage thresholds.

Figure 13 shows the results of the damage testing, where samples damaged at various power densities. Four discrete bars are listed for each sample representing power levels that were tested in each quadrant. The solid vertical bars for each sample quadrant rise to a tested power level that did not damage the optic. A solid red box in a quadrant represents the power level where failure occurred, at which point testing on the sample was stopped.

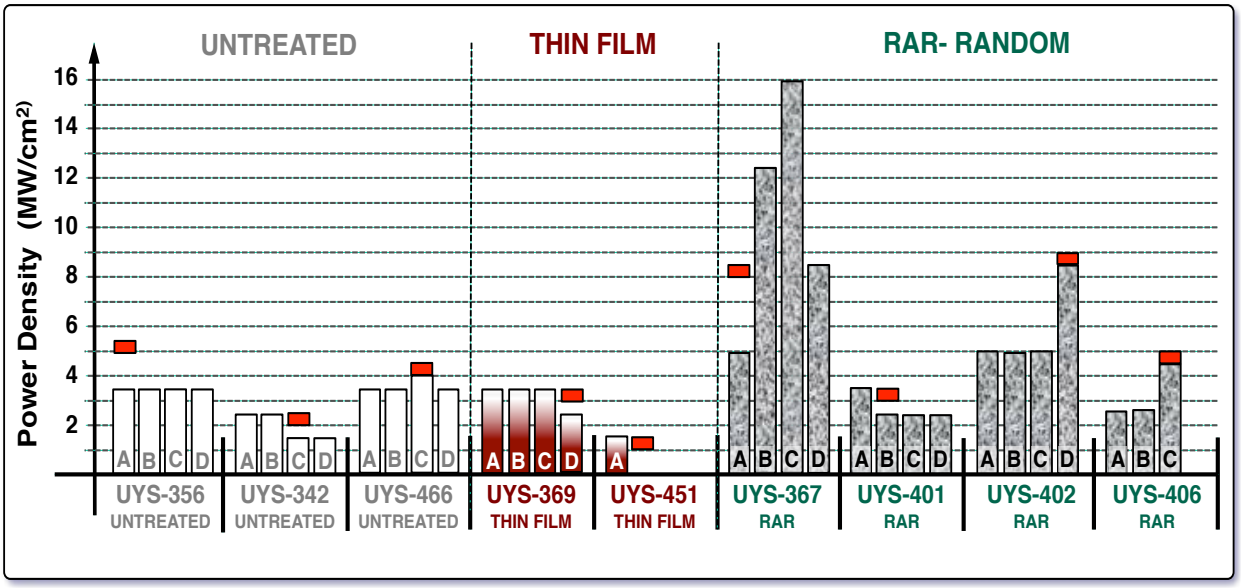


*Figure 13: Bar chart of CW laser damage testing of untreated, thin-film coated, and RAR textured YAG, with power density test levels shown for the 4 scanned quadrants on each sample.*

The data is somewhat scattered for a couple of reasons. First, CW laser damage to single crystal YAG is catastrophic, resulting in the optic fracturing as shown in the damaged YAG sample on the right. Once damage occurs, no more testing on the optic is possible. This is in contrast to pulsed laser damage testing where hundreds of sites may be tested with dozens of failures, allowed for data fitting to produce accurate damage thresholds. Secondly, the combination of the small power step increments taken and several RAR textured samples surviving longer than expected, resulted in a need to jump power levels to stay within time and budget limitations.


Damage at 1.0 MW/cm²

In summarizing the YAG damage data of Figure 13, if the maximum power density survived without failure in any quadrant at that power level is considered a threshold estimate- the untreated YAG showed a CW damage threshold of 2.5 MW/cm$^2$, which is in line with expectations in a scanning test with large sampling area. For the thin-film coated YAG, sample UYS-493 did not survive any power level, but if the sample is assigned the minimum test level of 1 MW/cm$^2$ threshold, the two sample coating threshold could be considered lass than 1.5 MW/cm$^2$. The RAR textured YAG samples survived to much higher powers so jumping levels or ramping power in just one quadrant was required. The average power density survived was unexpectedly high at 5.4 MW/cm$^2$, over 2x the untreated YAG. Typically, thin-film coatings result in lower damage thresholds for both pulsed and CW testing, such that the untreated sample thresholds are the target goal for any surface AR treatment.

Looking closer at the scattered results for the RAR samples, UYS-367 was 4-quadrant tested up to 4.5 MW/cm$^2$ without failure. Quadrant B of this sample was then stepped in 0.5 MW/cm$^2$ increments up to 9.0 MW/cm$^2$, with additional jumps to 10.0 and 12.0 MW/cm$^2$, where heating was finally observed and testing was stopped before damage occurred. Quadrant C was then jump ramped in three steps to maximum power density at 15.5 MW/cm$^2$ without damage or excessive heating. Jumping from 4.5 MW/cm$^2$ to 8.0 MW/cm$^2$ in quadrant D showed no issues, but jumping to 8.0 MW/cm$^2$ in quadrant A finally resulted in fracture damage. RAR treated sample UYS-402 was 4-quadrant tested to 4.5 MW/cm$^2$, then quadrant D was ramped in 0.5 MW/cm$^2$ steps until failure at 8.5 MW/cm$^2$. RAR samples UYS-401 and UYS-406 damaged at lower levels of 3.0 and 4.5 MW/cm$^2$ respectively.

While no definitive CW laser damage thresholds can be made from this study, the RAR textured YAG shows a significant and convincing CW laser damage threshold improvement to unexpected levels, however there isn't an obvious explanation for why the presence of a surface texture could reduce thermal failure mechanisms over an untreated part. It is possible that RAR etch post-bake at 480°C could be a complimentary part of the solution for increasing the CW laser damage of YAG. It seems clear however, that consistent with prior research, thin film AR coatings degrade the CW damage threshold of undoped YAG; while this study demonstrates that the RAR texture process provides a significant improvement in power handling. More detailed and statistically meaningful study is required to decouple the variables that could affect the CW laser survivability of undoped single crystal YAG, such as bulk absorption homogeneity in substrates, high temperature annealing, thermal conditioning during test, and other material and testing considerations.

## 8.0 SUMMARY

Surface relief AR nano-textures have been integrated into the surfaces of fused silica and yttrium aluminum garnet (YAG) laser components as a replacement for thin-film antireflection coatings for high power continuous wave (CW) laser applications. A series of 1070nm CW laser damage tests at 1070nm demonstrated that RAR textured fused silica optics could not be damaged up to the maximum power density of 15.5 MW/cm$^2$. Thermal imaging at maximum irradiance showed minimal laser induced heating of RAR textured samples, similar to results seen with untreated fused silica. In contrast to these results, the thin film coated samples show widely variable damage thresholds as low as 1 MW/cm$^2$, and thermal measurements revealed occasional spikes in temperature up to hundreds of degrees Celsius prior to failure. The CW damage results are attributed to levels of surface absorption for each AR treatment. Photothermal Common-path Interferometry (PCI) measurements showed no evidence of surface absorption for RAR textures, consistent with the absence of deposited materials. The thin film AR coatings exhibited surface absorption levels of 2-5 ppm, as well as the presence of large absorption spikes across the surface, which are attributed to coating defects. These absorption "hot spots" are considered to be precursors to failure for coatings as they exhibit extreme localized heating under high fluences, which can lead to failure at unpredictable levels. In a complimentary test under similar scanning conditions, untreated, RAR textured, and AR thin-film coated yttrium aluminum garnet (YAG) was CW laser damaged tested at 1070nm. The YAG substrates were undoped, precision polished (111) oriented single crystal material obtained from Synoptics. CW laser tests results show over 2X increase in damage threshold for RAR treated samples over untreated YAG, and over 3X increase over thin-film AR coated YAG. More detailed study is recommended to decouple the variables that show the RAR nano-texturing process for YAG significantly improved the CW damage threshold over as-polished YAG substrates.

## 9.0 ACKNOWLEDGEMENTS

The authors gratefully acknowledge the High Energy Laser, Joint Technology Office (HEL-JTO) for funding for the CW laser damage effort under contracts FA9451-12-D-0196 and FA9451-15-D-0019. MIT Lincoln Labs provided critical technical and material support throughout the multi-year effort. Detailed PCI absorption scans and data analysis was provided through the services of Chris Franz and Alexei Alexandrovski at Stanford Photothermal Solutions (SPTS). Raytheon Space and Airborne Systems of El Segundo CA contributed high quality YAG substrates and insightful technical discussions. The authors also thank Chris Varney of the Department of Physics and Astronomy at Washington State University for providing valuable insight on YAG color centers and annealing techniques.

## 10.0 REFERENCES


[1] Lowdermilk, W. H., Milam, D., "Graded-index antireflection…., " Appl. Physics Letters, **36** (11), 891 (1980)
[2] Hobbs, D. S., MacLeod, B. D., "High laser damage…. micro-structures.., " Proc. SPIE, **6720**, 67200L (2007)
[3] Hobbs, D.S., "Laser damage threshold measurements of anti-reflection microstructures operating in the near UV and mid-infrared, " Proc. SPIE **7842**, 78421Z (2010)
[4] Hobbs, D.S., et.al., "Laser damage resistant anti-reflection microstructures in Raytheon ceramic YAG, sapphire, ALON, and quartz, " Proc. SPIE **8016**, 80160T (2011)
[5] Hobbs, D. S., MacLeod, B. D., Sabatino, E., "Continued advancement of laser damage resistant optically functional microstructures, " Proc. SPIE **8530**, 85300O (2012)
[6] Bernhard, C., "Structural and functional adaptation in a visual system, " Endeavour **26**, 79 (1967)
[7] Clapham, P., Hutley, M., "Reduction of lens reflexion by the Moth Eye principle, " Nature **244**, 28 (1973)
[8] Wilson, S.J., and Hutley, M.C., "The optical properties of 'moth eye' antireflection…," Optica Acta **29**, (1982)
[9] Raguin, D.H., and Morris, G.M., "Antireflection structured surfaces…, " Applied Optics **32**, 7 (1993)
[10] Lalanne, P.; Morris, G., "Antireflection behavior of silicon subwavelength…., " Nanotechnology **8** (1997)
[11] Hobbs, D.S., et. al., "Automated Interference Lithography Systems for …..., " Proc. SPIE **3879**, 124 (1999)
[12] Hobbs, D. S., MacLeod, B. D., "Design, Fabrication, and Measured Performance of Anti-Reflecting Surface Textures in Infrared Transmitting Materials, " Proc. SPIE **5786**, 349 (2005)
[13] Hobbs, D. S., MacLeod, B. D., "Update on the Development of High Performance Anti-Reflecting Surface Relief Micro-Structures, " Proc. SPIE **6545**, 65450Y (2007)
[14] Chhajed, S. et al, "Nanostructured multilayer graded-index antireflection coating for Si solar cells with broadband and omnidirectional characteristics, " Applied Physics Letters **93**, 251108 (2008)
[15] MacLeod,B.D., Hobbs,D.S., "Long life, high performance anti-reflection…," Proc. SPIE **6940**, 69400Y (2008)
[16] MacLeod, B.D., et.al., "Moldable AR microstructures for ….. CIRCM …., " Proc. SPIE **8016**, 80160Q (2011)
[17] Liu, B., Yeh, W, "Antireflective surface fabricated from colloidal…., " Colloids and Surfaces A, 356 (2010)
[18] Rahman A., "Sub-50-nm self-assembled nanotextures for enhanced broadband antireflection in silicon solar cells", Nature Communications **6**, 5963 (2015)
[19] Alexandrovski, A., et. al., "Photothermal common-path interferometry….." Proc. SPIE **7193**, 71930D (2009)
[20] Clark, C., et. al., "Comparison of Single-Layer and Double-Layer Anti-Reflection Coatings Using Laser-Induced Damage Threshold and Photothermal Common-Path Interferometry", Coatings 6, 20, (2016)
[21] Hobbs, D. S., et.al., "Contamination resistant antireflection nano-textures.., " Proc. SPIE, **8885**, 88850J (2013)
[22] Varney, C.R., and Selim, F.A., "Color Centers in YAG, " AIMS Material Science **2**, Issue4 (2015)